Circle-like foreign element detection using normalized cross-correlation and unsupervised clustering in CXR image

Fatema Tuz Zohora[a], K.C. Santosh[a], and Sameer Antani[b]

[a]Dept. of Computer Science, The University of South Dakota, Vermillion, SD 57069
[b]US National Library of Medicine, NIH, 8600 Rockville Pike, Bethesda, MD 20894

ABSTRACT

In this paper, we present a new technique to detect circle-like foreign elements within chest X-ray (CXR) images. In our technique, we use a pre-processing step that enhances the CXR images to increase the contrast between the circle-like elements with their background, using intensity normalization and image adjustment. Using these enhanced images, we then perform normalized cross-correlation (using positive and negative templates) and unsupervised hierarchical clustering for foreign element detection. Additionally, we automate our system for comparing annotated ground-truths of test dataset with corresponding detection results and hence measuring detection performance of circle-like foreign elements. We also compare our proposed technique with existing techniques in the literature (i.e., candidate selection followed by circular Hough transform (CHT), ViolaJones, and CHT). In all such tests, our proposed novel technique is able to excel in performance in terms of detection accuracy - precision(90%), recall(93%), and F1 score(91%).

Keywords: chest X-ray (CXR), foreign element detection, circular Hough transform (CHT), normalized cross-correlation (NCC), unsupervised hierarchical clustering, Viola-Jones

1. DESCRIPTION OF PURPOSE

Lung diseases are one of the major health threats in current time. Every year a large numbers of people suffer from various lung diseases, such as tuberculosis 1, pneumonia, lung cancer, and pulmonary edema, across the world. The advent of new powerful hardware and software techniques for lung disease detection has triggered attempts to develop computer-aided diagnostic (CAD) systems for automatic chest x-ray screening 2. However, foreign elements, such as buttons on the gown that the patients were wearing or coins/buttons mistakenly swallowed by patients, within the chest x-ray images (especially the ones located within the lung region) hinder the CAD system performance, as they are not due to any lung abnormalities and therefore should not be considered. Therefore, in the screening process precise detection of foreign element is an important issue for screening of chest diseases in CAD systems. Fig. 2-a shows one such CXR which contains several circle-like elements.

Detecting foreign element in CXRs is a challenging and open research problem. There are only few works in the literature that try to tackle this problem 3, 4, 5. Such techniques are Viola-Jones, CHT, and candidate selection (CS) followed by CHT. Among them, CHT and candidate selection followed by CHT both have average recall and precision rate and their performance depends on the image intensity. If there is not enough contrast between the objects (circle-like element in CXRs) and the background image, then the performance of CHT degrades drastically. On the other hand, Viola-Jones algorithm has high false detection rate, which is confusing for the CAD systems. For improving CAD systems, more precise methods are required. And in this paper we present such a precise technique based on normalized cross-correlation and unsupervised clustering.

2. METHODS

In our proposed technique, we first enhanced the CXR images to increase the contrast between the circle-like elements with their background, using intensity normalization and image adjustment. Next, we apply normalized cross-correlation to find the cross-correlation coefficient with positive and negative template. For computing the centre of the circle-like foreign element, we then performed unsupervised clustering. Fig. 1 briefly presents the proposed method work-flow.

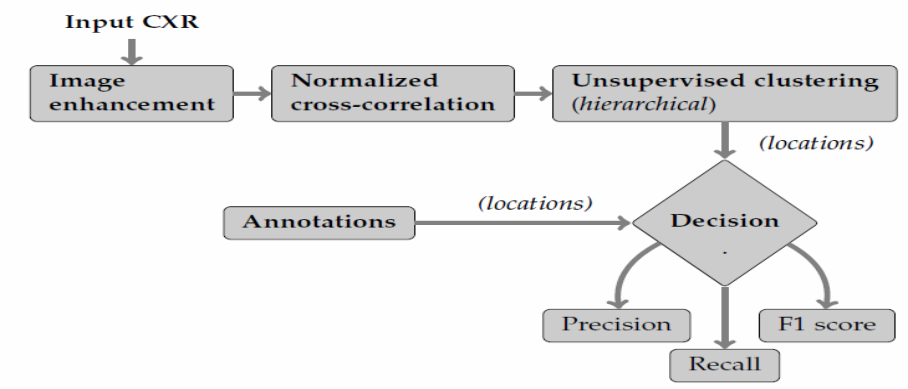

Figure 1. Work-flow.

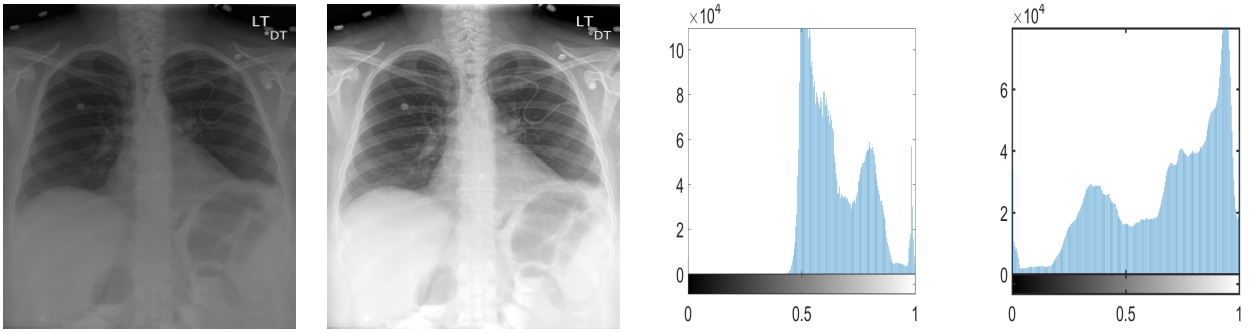

a) Original CXR b) Enhanced CXR c) Original histogram d) Enhanced histogram

Figure 2. Image enhancement of input chest X-ray image.

2.1 Image enhancement

We applied some pre-processing steps on the CXRs to improve the image quality, so that the objects of interest (e.g., circle-like elements) become more evident. The quality of the pre-processing steps strongly affects the performance of the subsequent detection steps. In our tests, we applied two pre-processing steps: intensity normalization and image adjustment. For both steps, we used the same approach as in 4, 5. Fig. 2 shows one such low contrast input and the resultant image after enhancement respectively. It also shows the histogram of pixel intensities before and after the adjustment. It can be seen from the figure that the adjusted image has more uniformly distributed intensity values and a higher contrast.

2.2 Normalized cross-correlation

After enhancing the input CXRs, we performed template matching on them to detect circle like foreign elements. To improve the performance of template matching we also tried segmenting the lung area and performing the matching only on the segmented area. For lung segmentation, we applied anatomical atlases with nonrigid registration algorithm in 6. In Section 3 we show comparison of detection performance both with or without lung segmentation.

For robust template matching, zero-mean normalized cross-correlation (NCC) was used in our system. It is defined as:

$$C(x_0, y_0) = \frac{1}{N} \sum_{x,y} \frac{(I(x_0 + x, y_0 + y) - \overline{I}(x_0, y_0))(T(x, y) - \overline{T})}{\sigma_{I(x_0,y_0)} \sigma_T}, \tag{1}$$

where $C(x_0, y_0)$ is the NCC coefficient between template T and image I at pixel (x_0, y_0). Here N is the total number of pixels in T, $\overline{I}(x_0, y_0)$ and $\overline{T}$ are corresponding means, and $\sigma_{I(x_0,y_0)}$ and σ_T are corresponding standard deviations of the image region and the template. For an efficient implementation of NCC, we used integral images to compute mean and standard deviation. For computing the cross-correlation coefficients efficiently, we took

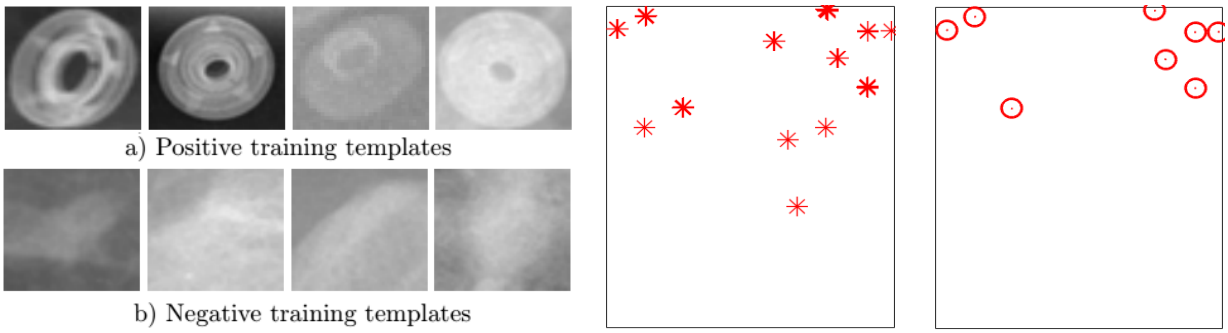

a) Positive training templates

b) Negative training templates

c) Final NCC output

d) Final clustering output

Figure 3. Sample positive and negative templates, final NCC output, and final clustering output respectively.

advantage of the convolution theorem * and performed correlation in the frequency domain. To do so we flipped the template 90 degree counter clock-wise, took 2D FFT of both the input image and the flipped template, and then performed inverse FFT on the element-wise product of the two FFT signals.

For robust detection, we performed template matching using both positive and negative templates. In our tests, we chose templates of size 82×82. For each template, after performing cross-correlation we eliminated the correlation scores that are below a threshold. For positive templates the threshold is chosen to be max(0.32, 5th highest NCC value in the image) and for negative templates the threshold is chosen to be 0.32. After thresholding the remaining NCC scores are accumulated in a score matrix, accumulated_score = max(accumulated_score, new_score). Finally, the score matrices formed by the positive and the negative templates are compared and a binary detection mask is created by marking the pixel locations where the positive score is higher than the negative score (shown in Fig. 3-c).

2.3 Unsupervised clustering

After getting the detection mask from NCC, we performed unsupervised clustering to detect spatial clusters in the mask. For clustering we used an agglomerative/bottom up hierarchical approach, where every data starts in its own cluster, and two clusters are combined as one advance the hierarchy. While combining clusters, a radius of 26 pixel is used. Next, we removed any cluster for which the number of elements is smaller than a threshold. Finally, we calculated the mean of each remaining cluster and marked it as the center of the detected circle-like object. Fig. 3-d, shows the final clustering output.

3. RESULTS

In our experiments, we used a subset of dataset maintained by National Library of Medicine (NLM) - National Institutes of Health (NIH), which is composed of 400 DICOM images where there are total 325 circle-like elements within the lung area and 1178 overall. When computing the experimental results, we used precision, recall, and F1 score for evaluation metrics. For observing the experimental results of our test dataset, we used k-fold (k=10) cross-validation where the dataset is randomly segmented into k same sized sub partitions.

The detection performance of our proposed technique is presented in Tables 1 with and without lung segmentation. Here we only presented the average detection performance of our 10-fold cross validation. Fig. 4-a, shows the resultant output without lung segmentation. It can be seen from the figure that there are no false detection or undetected circle-like elements. Using our proposed technique, the detection performance was high across all images in the dataset.

Next, we compared our NCC based hierarchical clustering technique with three other techniques in the literature: Candidate selection followed by CHT (CS with CHT), CHT, and Viola-Jones, presented in 3, 4. Compared to our approach, Viola-Jones suffer from low precision due to large number of positive training samples that leads to false detection. On the other hand, CHT with CS and CHT has poor recall without lung segmentation. Fig. 4-b, c, and d show the resultant output of CS with CHT, CHT, and Viola-Jones respectively.

*The point-wise product of Fourier transforms is the Fourier transform of convolution.

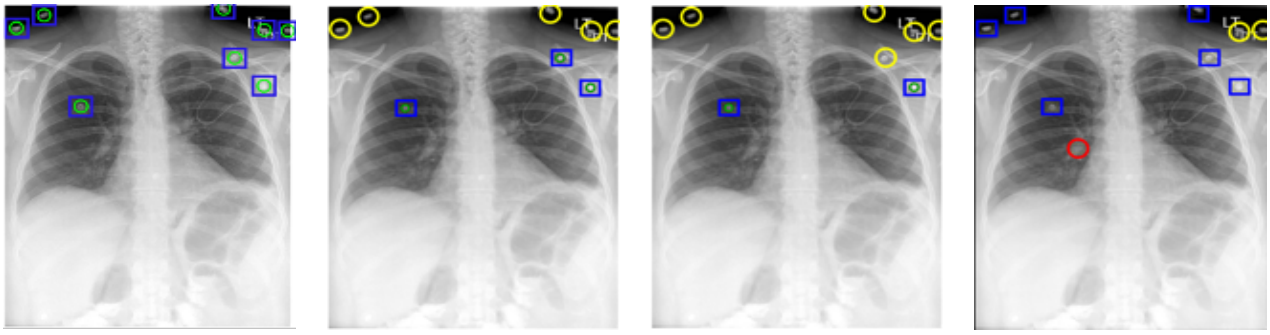

a) NCC with clustering b) CS with CHT c) CHT d) Viola-Jones

Figure 4. Circle-like element detection: a) NCC with hierarchical clustering, b) CHT with CS, c) CHT, and d) Viola-Jones. Here, yellow circles indicate false negative (un-detected elements), red circles indicate false positive (inaccurately detection) and blue rectangles indicate true positive (accurate detection).

Table 1. Comparison of circle-like foreign element detection result

Techniques	with lung segmentation			without lung segmentation		
	Precision	**Recall**	**F1 score**	**Precision**	**Recall**	**F1 score**
NCC with clustering	0.90	0.93	0.91	0.76	0.88	0.81
CHT with CS	0.96	0.90	0.92	0.85	0.54	0.66
Viola-Jones	0.36	1	0.52	0.37	0.94	0. 53
CHT	0.94	0.74	0.83	0.81	0.45	0.58

4. CONCLUSIONS

In this work, we have focused on identifying circle-like foreign elements in CXR images such as buttons appearing in the chest X-ray images. We have presented a novel technique for circle-like foreign element detection. Our proposed technique, normalized cross-correlation (NCC) followed by an unsupervised clustering is encouraging, in terms of detection accuracy - precision, recall, and F1 score. Our proposed technique performed robustly under a variety of dataset even without lung segmentation. We can see from our results that using our proposed technique, we can get 90% (76%), 93% (88%), and 91% (81%) precision, recall, and F1 score respectively with lung segmentation (without lung segmentation). As future work, we plan to extend this work to detect other types of non-circular foreign element (e.g., medical tubes) that usually appears in CXRs.

REFERENCES

[1] WHO, "World Health Organization (WHO),: global tuberculosis report," (2014).

[2] Santosh, K., Vajda, S., Antani, S., and Thoma, G. R., "Edge map analysis in chest x-rays for automatic pulmonary abnormality screening," *International journal of computer assisted radiology and surgery* , 1–10 (2016).

[3] Xue, Z., Candemir, S., Antani, S., Long, L. R., Jaeger, S., Demner-Fushman, D., and Thoma, G. R., "Foreign object detection in chest x-rays," in [*Bioinformatics and Biomedicine (BIBM), 2015 IEEE International Conference on*], 956–961, IEEE (2015).

[4] Zohora, F. T. and Santosh, K., "Circular foreign object detection in chest x-ray images," in [*International Conference on Recent Trends in Image Processing and Pattern Recognition*], 391–401, Springer (2016).

[5] Zohora, F. T. and Santosh, K., "Foreign circular element detection in chest x-rays for effective automated pulmonary abnormality screening," 36–49 (2017).

[6] Candemir, S., Jaeger, S., Palaniappan, K., Musco, J. P., Singh, R. K., Xue, Z., Karargyris, A., Antani, S., Thoma, G., and McDonald, C. J., "Lung segmentation in chest radiographs using anatomical atlases with nonrigid registration," *IEEE transactions on medical imaging* **33**(2), 577–590 (2014).